

# Background Removal for the Processing of Scans Acquired with the “UGO-1<sup>st</sup>” Landmine Detection Platform

L. Capineri<sup>1</sup>, P. Falorni<sup>1</sup>, G. Borgioli<sup>4</sup>, L. Bossi<sup>1</sup>, G. Pochanin<sup>2</sup>, V. Ruban<sup>2</sup>,  
O. Pochanin<sup>2</sup>, T. Ogurtsova<sup>2</sup>, F. Crawford<sup>3</sup>, and T. Bechtel<sup>3</sup>

<sup>1</sup>University of Florence, DINFO, Italy

<sup>2</sup>Usikov Institute for Radiophysics and Electronics  
National Academy of Sciences of Ukraine, Ukraine

<sup>3</sup>Franklin and Marshall College, PA, USA

<sup>4</sup>University of Florence, DIMAI, Italy

**Abstract**— Field tests of the robotic platform “UGO-1st” have revealed interference sources that complicate the automatic detection of subsurface objects by UWBGPR. Although robust target discrimination criteria make it possible to reduce the probability of false alarms, identification of these sources of interference improves the detection algorithm. The focus of this work is on the elimination of interference sources, which include: direct coupling between radar antennas; reflections from components of the robotic platform; reflections from the soil surface; instability of the GPR signal due to temperature drift during a scan.

To reduce these effects we performed measurements with the robotic system suspended in air high above the ground so that signals from any subsurface reflection would arrive long after the signals from the robot structure that are to be identified and removed. These signals are also used to compensate for temperature drift, as well as to remove signals from direct coupling between antennas

The procedure for the background removal includes: selection of a time window before the reflection from surface; an optimization procedure for determining the time drift caused by temperature changes; alignment of the two signals; and subtraction of the background signal from the received one. This is performed for all four receiving channels separately. The need to remove reflections from the soil surface is due to the fact that these signals arrive at the receiver almost simultaneously with the reflections from shallow buried objects. This makes it difficult to determine the arrival time of the reflected signal. Reflections from the soil surface can also be eliminated in a manner similar to the one mentioned above but instead of measuring a background signal we took signals collected a few cm ahead of a known target. The algorithm was applied to real data and has proven to be effective.

## 1. INTRODUCTION

The use of ultra-wide-band ground penetrating radar (UWBGPR) with an array of antennas mounted on a robotic platform [1], for the purpose of discriminating buried mine-like targets [2], requires a careful analysis of all possible causes of interference and pulse reverberation from the environment and from the metallic structure of the robotic vehicle. Fig. 1 shows the system components on the platform.

Regarding the interference of the UWBGPR from other RF devices operating in the vicinity, an experimental test of the significance of this effect was carried out in a systematic way. The RF devices active during the acquisition of signal with the UWBGPR are listed below:

1. 2 GHz Holographic Radar (HSR).
2. WiFi access point.
3. Bluetooth remote control.

For the test of the susceptibility of the sensor to these sources of interference, the four receiving channels of the UWBGPR were continuously displayed on the remote PC with maximum gain. Each of the three RF devices was switched on and off sequentially to check for any modification of the four received signals. The result was that no significant variations were observed and we conclude that in the configuration shown in Fig. 1 the UWBGPR is not subject to significant external or stray interference.

The two radars operate at distances from the ground surface that are about 32 cm for the UWBGPR and a distance of between 5 and 15 cm (programmable) for the holographic radar. These

distances are imposed to avoid the collision of the antennae with irregular ground, vegetation or possibly tripwires. Moreover, the adjustable distance from the ground can mitigate the effects of some types of irregularities on the holographic images [3]. Other approaches to mitigate the surface irregularities in microwave holograms are proposed in [4]. The Picoflexx camera provides a realtime distance map and optical image to the remote terminal for the driver (field operator) of the robotic platform. This operating condition for the two radars is quite different from standard GPR systems that have the antenna well-coupled to the ground.

When the radar signal reaches the air-soil interface, it scatters in all directions. From experiments, we found that in some cases the HSR reflections hit the metal frame of the mechanical scanner and bounce back to the antenna. This effect was evident in HSR images since this received signal is well-correlated with the spatial sampling performed with the mechanical scanner. Conversely, reflections from the metal frame were negligible for the front-looking, raised UWB Radar, because the antenna array is positioned on the front of the vehicle and located outside of the metal frame perimeter. One possible cause of interference from objects in the environment is from the presence of targets located just above the antenna array. Some back-reflected radiation is present and the high sensitivity of the four receiving channels picks up these reflected signals. To avoid such interference, no operator/driver or generic reflector should be present above the antenna at a distance smaller than 50 cm.

Investigation of all possible causes of interference indicated that there is a direct coupling between the five antennae of the array that prevents the detection of weak signals reflected from low-dielectric-contrast plastic targets. In Section 2.1 we describe the method we have adopted to evaluate this cause of interference and how it can be mitigated to improve target detection with the UWBGPR.

The detection of the target is performed by processing the four receiving channels from the antenna array while the robotic platform is moving on the ground. This movement (normally at a low speed, less than 5 cm/s) is made on an irregular surface that continuously changes the relative distance and central axis direction of the antenna array to the soil surface [5]. The embedded processing required to detect a buried target in real-time needs to be robust in order to avoid missing any targets with a radar cross section equivalent to a plastic or metal-cased landmine. The explanation of the adopted method is reported in Section 2.2, the algorithm is described in Section 3, and the experimental results are given in Section 4.

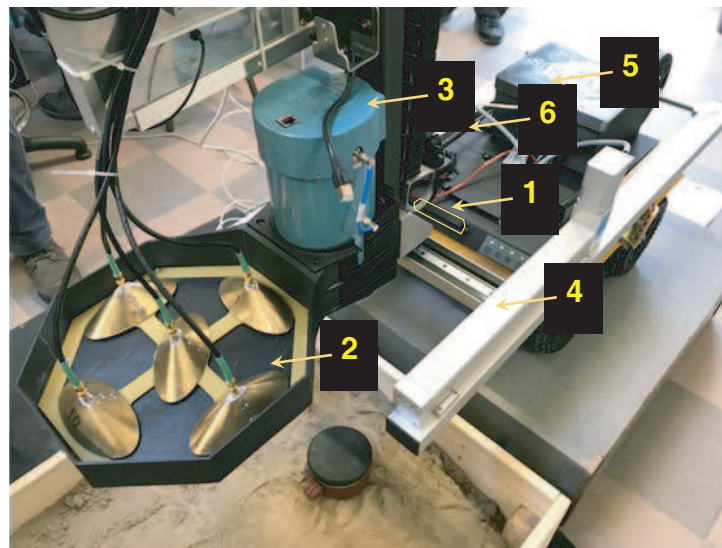


Figure 1: Robotic platform components/devices: 1) Picoflexx 3D camera, 2) UWBGPR; the central antenna is the transmitter ( $T$ ), the four receiving antennae ( $R$ ) are at  $90^\circ$  angular spacing, 3) HSR, 4) Mechanical scanner (FESTO, Germany), 5) electronic control and data acquisition box with Blue Tooth Connection, 6) WiFi access point.

## 2. RADAR SIGNAL PROCESSING FOR SHALLOW TARGET DETECTION WITH THE UWBGPR AND 1T+4R ANTENNA SYSTEM

### 2.1. Method Used to Reduce the Interference Originating from the Direct Coupling between the Transmitting and Receiving Antennas and Reflections from the Robotic Platform

Despite the directivity inherent in the antenna used [6], there is a significant part of the signal that propagates toward the platform and reflects back to the receiving antennas. Since the dielectric contrast of objects of interest (such as small plastic-cased landmines) is small these self-reflections create significant clutter that masks reflections from target objects. In order to eliminate this clutter we must record it and subtract these signals from the received waveform.

Since the objects of interest are buried at shallow depths (e.g., 3 cm) and the antenna system is at a height of 32 cm above the surface of the soil, the time window containing the reflections from the objects has duration of about 5 ns to 6 ns. To record a clear background signal we lifted the robotic platform to a height of 1.4 m and recorded signals in all four receiving channels. In the next section, only data from the first channel of the four are presented but all were analysed.

Radars for humanitarian demining must work properly in variable weather conditions. This means that time drift from temperature changes must be eliminated. We use an adjustment method to address this problem.

Figure 2(a) shows the signal background (BG) received by the first channel of the antenna system. This signal contains the electromagnetic coupling between the radiating and receiving antennas and reflections from elements of the antenna system and robotic platform. We then collected data in the test field for shallow buried metal tin, inert PMN-1 and PMN-4 mines.

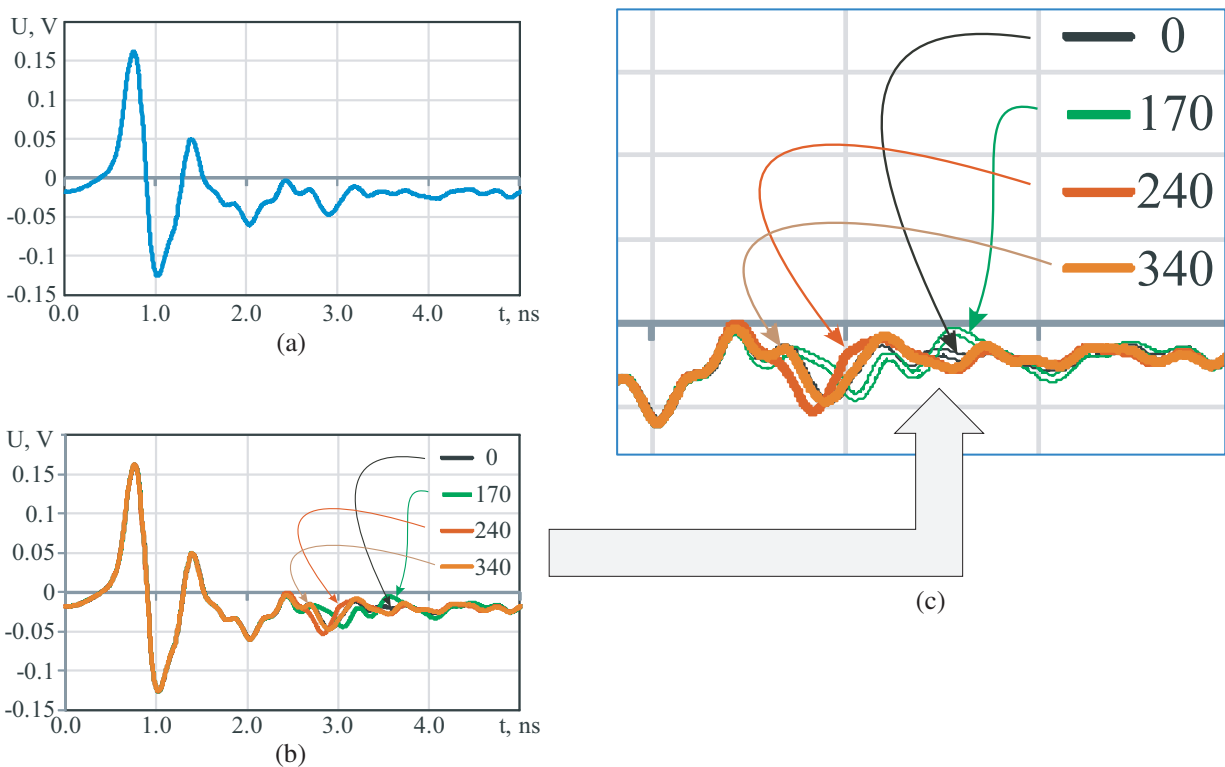


Figure 2: (a) Background signal, (b) 0th no object, 170th signal (with metal tin), 240th signal (with inert PMN-4 mine), 340th signal (with inert PMN-1 mine), signals received by the first channel, (c) magnified plot with reflections from objects.

As we can see in Fig. 2(b), the impulse due to coupling between the antennas is the earliest and largest signal. We subtract the BG signal from the signals received by the 1st channel in the four positions sequentially (without object and with three objects) according to the following three steps processing algorithm:

1. We define the time interval in which the only BG is present and its form is repeated in the signal received in the 1st channel. In the calculations presented the time interval consists of 250 samples with sampling time 10 ps.

- Next, we determined how much to shift the signal currently received by the 1st channel with respect to the BG signal. To do this we find the minimum of the function.

$$g(k) = \frac{1}{M+1} \sum_{i=0}^M (B_i - S_{i+k})^2, \quad k = 0 \div N. \quad (1)$$

In (1)  $M$  is the number of samples in the time interval (e.g.,  $M = 250$ ) at which we compare the main part of the BG signal with the main part of the signal in the first channel;  $N$  is the whole number of steps necessary for the waveforms of the BG and component of background in the signal of the first channel to coincide. When  $g(k)$  reaches a minimum it means that at the time shift corresponding to  $k$  steps the two waveforms are coincident. These signals are shown in Fig. 4. A plot of the dependence  $g(k)$  for the 240th signal is shown in Fig. 3. In this case, in order to adjust two waveforms the signal in the first channel must be shifted at  $k = 4$  steps to the left.

- After the signal has been shifted by the required number of steps, it becomes possible to almost entirely subtract BG from the received signal (Fig. 4).

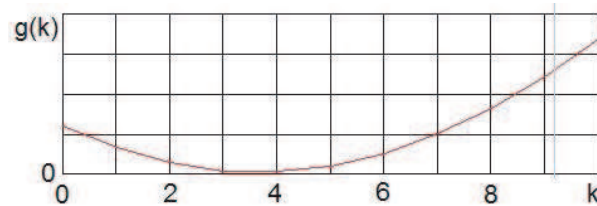


Figure 3: The required time shift corresponds to  $k$  where  $g(k)$  is at a minimum.

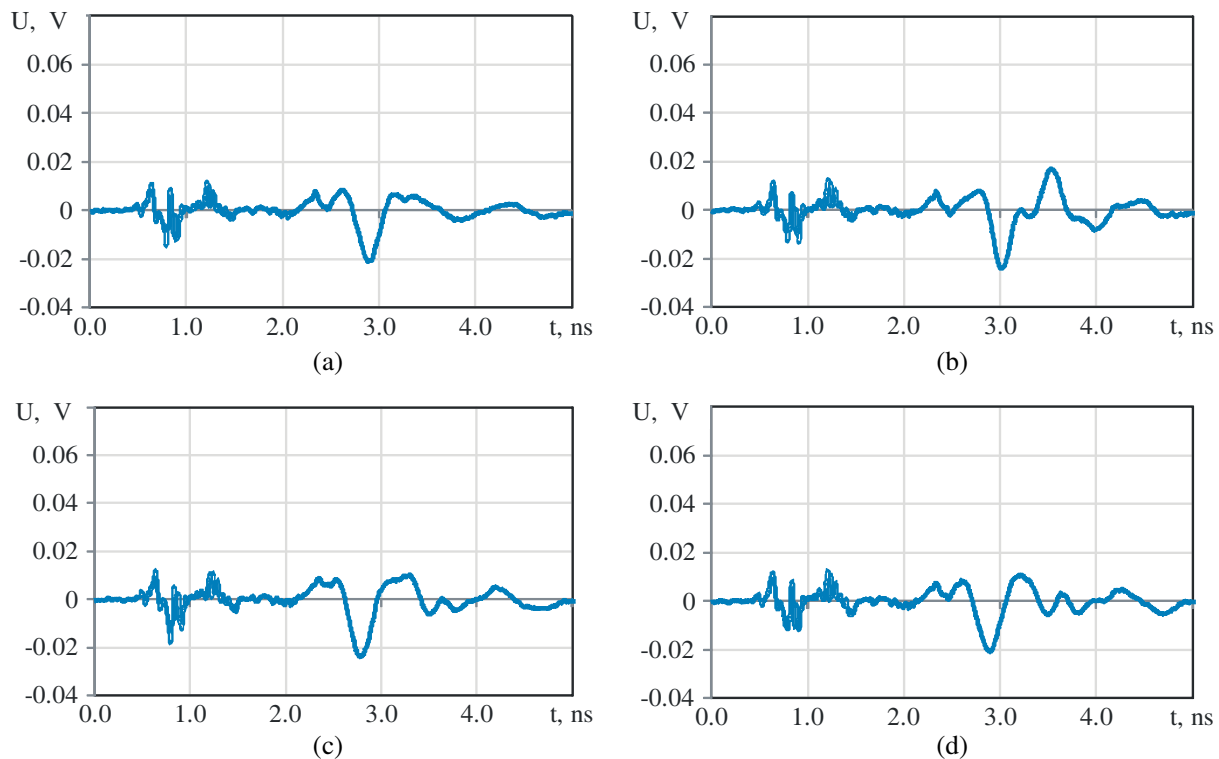


Figure 4: (a) 0th signal, (b) 170th signal (with metal tin), (c) 240th signal (with PMN-4), (d) 340th (with PMN-1) signal after adjusted subtraction of direct coupling and other reflections from metal frames.

## 2.2. Method for Surface Reflection Removal

Consider the 1T+4R antenna system as a tetrad of bistatic antenna systems: T-R1, T-R2, T-R3, T-R4. The first recorded signal by each of the bistatic pairs is the surface reflection ( $SR(t)$ ), where  $t$  is the current time. After a short time interval the object reflection ( $OR(t)$ ) arrives at the receiving antenna. As a result the radar records an output signal  $OS(t) = SR(t) + OR(t)$ . If the signals  $SR(t)$  and  $OR(t)$  are overlapped in time, the waveform of  $OS(t)$  becomes very difficult to use for target recognition using Pearson's correlation [7]. Therefore, to discriminate  $OR(t)$  clearly, we need to do a subtraction  $OS(t) - SR(t)$ . For this aim, we record a reflection from an area, which is clear from any subsurface object. In the ideal case  $OS(t) = SR(t) + 0$ .

We apply an algorithm similar to that used for background removal. In this case the signal to subtract is the first recorded signal in the profile. The only assumption that we make is the absence of an object under the antenna system at the starting point.

In order to adjust the time position of the surface reflection from the soil, we apply the procedure using as a reference a portion of the signal #0 in the profile (for example, from 2.5 to 3.5 ns in Fig. 4(b)). Then we multiply the waveform being processed by a coefficient which is the ratio of the minimum amplitude of the surface reflection for the initial signal to the max absolute amplitude of the surface reflection for the current signal:  $\max ABS(U_1) / \max ABS(U_j)$ .

After the adjusted subtraction is performed, the processed signals look like those shown in Fig. 5. We add signal #80 which is not affected by the presence of a buried object. Unfortunately complete subtraction is rarely achieved because of the difference in waveforms around time 2.5 ns. At this time, some reflection from the surface still exists. However, the subtraction results in much cleaner signals than signals before subtraction (Fig. 5(a)). The reflections from objects in the time interval from 3 to 4 ns also become more clearly visible, and consequently this waveform is much simpler to process in the next step.

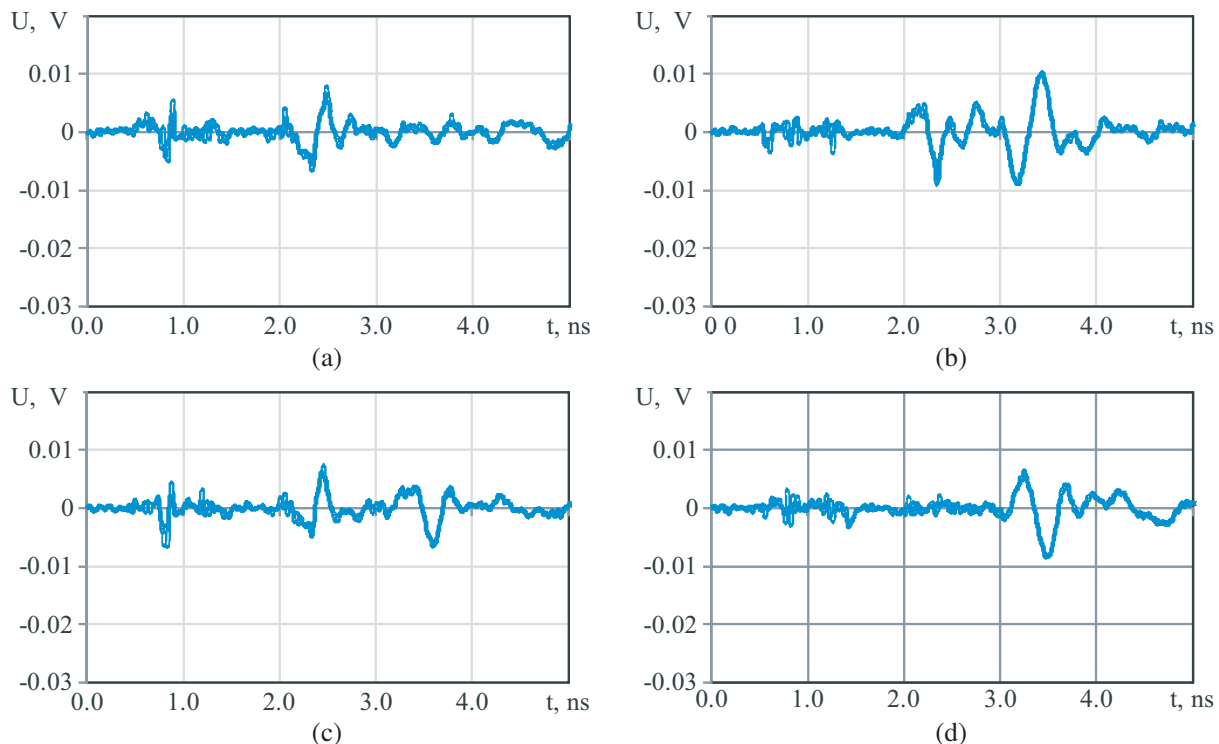


Figure 5: (a) 80th signal, (b) 170th signal, (c) 240th signal, (d) 340th after adjusted subtraction of soil surface.

Figure 5 shows waveforms reflected by soil without any object (Fig. 5(a)), metallic (Fig. 5(b)) and plastic (Figs. 5(c)–(d)) objects.

The next stage of data processing is the calculation of possible subsurface object coordinates [6, 8]. Then we find position of detected subsurface objects using the criteria described in [2].

### 3. ALGORITHM FOR DATA PROCESSING WITH BACKGROUND REMOVAL

Figure 6 shows the flowchart of the data processing algorithm.

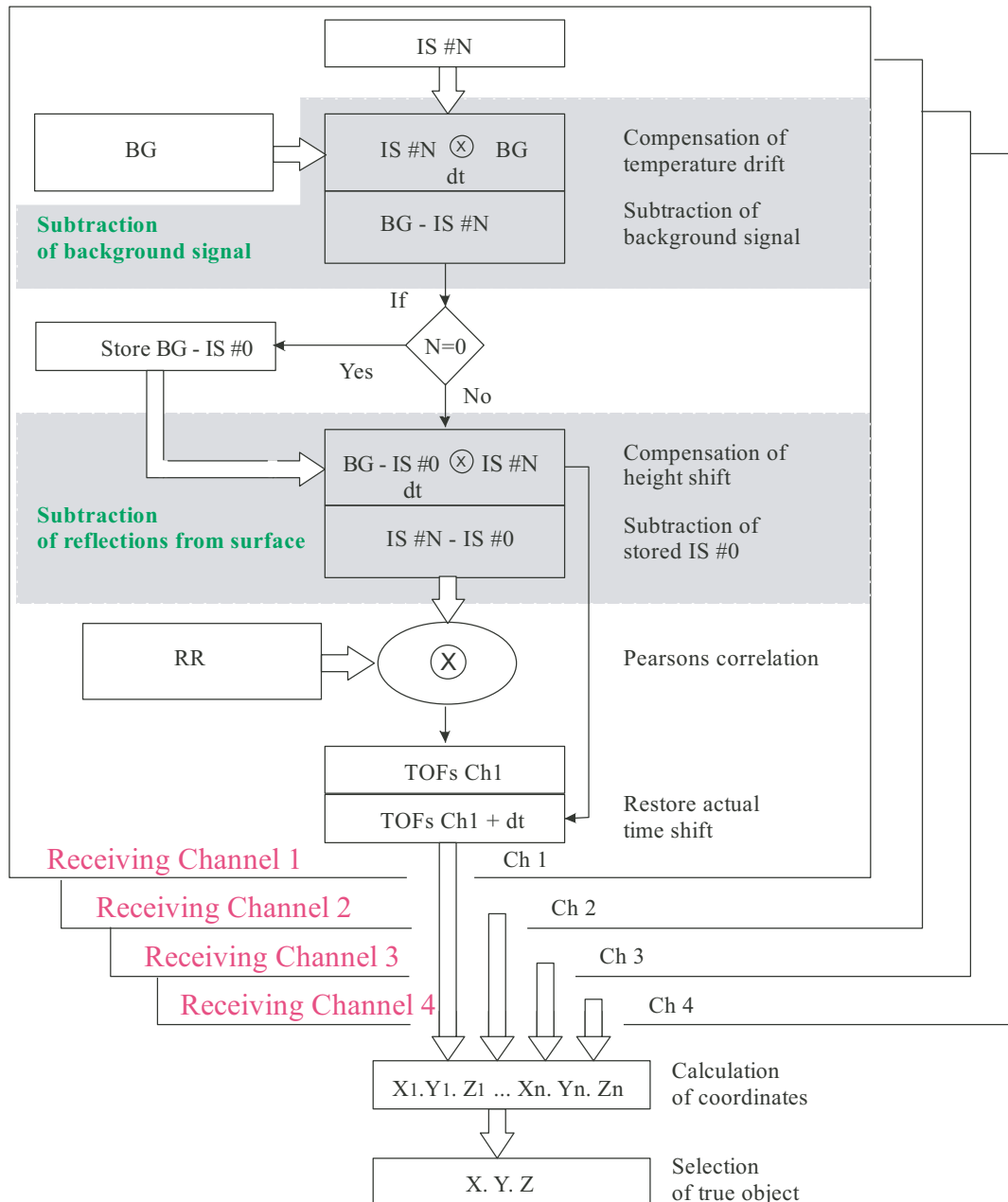


Figure 6: Data processing algorithm. The designations used in the figure are as follows:  $N$  is the quantity of receiving channels,  $Ch\#$  is number of the receiving channel,  $BG$  is the stored background signal,  $IS\#N$  is an input signal coming from the receiving channel  $\#N$ ,  $RR$  is a stored replica with a reflection from the surface.

The input signal from receiver  $\#1$  arrives from the 16 bit Analog-Digital Converter (ADC) at the input of “Subtraction of background signal” process (Fig. 6). The same procedure takes the  $BG$  signal from the processor memory and aligns it with respect to  $BG$  signal. The  $BG$  signal is then subtracted from the current signal. At the output of this procedure, we obtain a waveform without the background and with a compensated temperature drift.

Then we move to the “Subtraction of reflections from surface” procedure. First we store the signal  $\#0$  ( $SR(t)$ ) as a pattern for future subtraction. Starting from signal  $\#1$  we can process the data completely. This procedure takes the  $SR(t)$  signal from the processor memory. During this procedure the current signal is aligned with respect to  $SR(t)$  signal using (1) and the  $SR(t)$  signal

is subtracted from the current signal. At the output of this procedure, we obtain the waveform which is almost free of surface reflection and with a compensation for change in antenna height.

Next is the recognition of reflections by objects and the determination of their position. In our experiments the reflection from a metallic disk of diameter 12 cm was used as the pattern for correlation (RR). The detected Time of Flight (TOF) obtained for each of channel #1 through #4 are used as input data for the calculation of all 3 Cartesian coordinates of the subsurface object.

Since a large numbers of TOFs are usually measured in order not to miss any objects, we must use all combinations of them to calculate the coordinates of objects. Some of the coordinates correspond to real objects, but the rest of the coordinates do not. They are caused by random segments in the recorded waveform that are similar to the waveform used in the Pearson correlation. Therefore it is necessary to select real objects from clutter objects using a specifically developed spatial filter as described in [2]. The selection procedure gives all three coordinates of a detected subsurface object.

## 4. EXPERIMENTS

### 4.1. Test Site for Experiments

Experiments were done on the grounds of the University of Florence with three buried objects: a metal tin, and plastic landmine simulants of type PMN-4 and PMN-1. Experiments were conducted three months after the objects were buried. The thickness of the soil layer above the objects was about 3 cm. The length of test path was 2.6 m and the distance between the objects was 60 cm (Fig. 7).



Figure 7: Test field.

### 4.2. Results of Sounding Experiments

A measurement time scale of 5 ns was used. Fig. 8 shows a comparison of the results of the two approaches for data processing:

- 1) simple subtraction of signal #0 from all data acquired by channel 1;
- 2) adjusted subtraction of BG and surface reflections.

There are a few notable results in Fig. 8.

- All three objects are visible in all B-scans and are associated with hyperbolic patterns.
- Simple subtraction of signal #0 increases the contrast of object reflections (Fig. 8(b)). However, there are signals above the reflections from the objects that are quite strong, and these strong signals vary rapidly along the sounding path. Therefore, it is necessary to make data processing very sophisticated in order to detect all subsurface objects without producing false alarms.

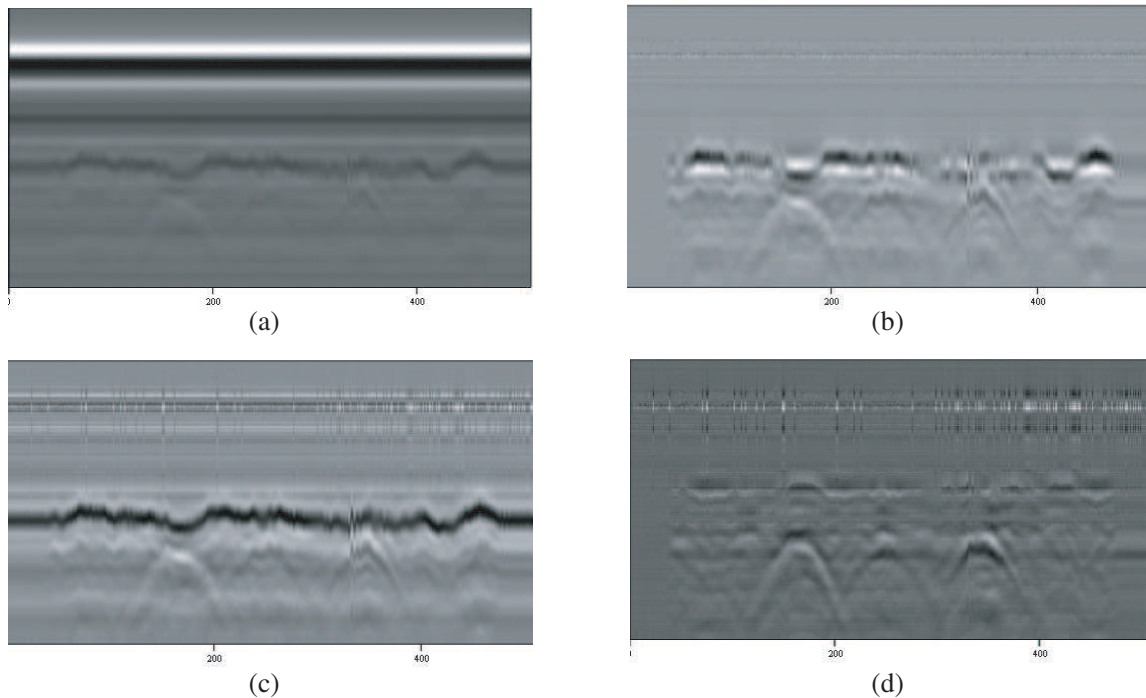


Figure 8: B-scan of Channel 1. (a) Raw B-scan; (b) Subtraction of signal #0; (c) Adjusted subtraction of background signal; (d) Adjusted subtraction of reflection from soil surface after adjusted subtraction of background signal.

- After adjusted subtraction of the background signal, the surface reflections have increased contrast. This makes it possible to estimate the range for the height change of the antenna during movement of the robotic platform during sounding.
- After adjusted subtraction, the surface reflections by subsurface objects become the more visible.

Thus, this provides a smaller total number of TOFs which are all related to real objects, and the probability of false alarm is trends towards 0, while the probability of detection approaches 1.

## 5. CONCLUSIONS

Owing to the adjusted subtraction of the background and the reflection from the surface we obtained two positive results:

1. We eliminated a strong background signal.
2. We obtained a better waveform of reflections from the surface of the soil.

After all subtractions were done, we had a more reliable Pearson's correlation and a simplification of the TOF determination

## ACKNOWLEDGMENT

The authors wish to acknowledge the funding of the NATO project G5014 "Holographic and Impulse Subsurface Radar for Landmine and IED Detection".

## REFERENCES

1. <http://www.nato-sfps-landmines.eu>.
2. Ogurtsova, T., et al., "Criteria for selecting object coordinates at probing by the impulse UWB GPR with the "1Tx + 4Rx" antenna system," *9th International Conference on Ultrawideband and Ultrashort Impulse Signals (UWBUSIS)*, 161–164, Odessa, Ukraine, 2018.
3. Qin, T., L. Bossi, A. Bartolini, P. Falorni, P. Giannelli, Y. Zhao, and L. Capineri, "Influence analysis of uneven surface on landmine detection using holographic radar," *2018 Progress In Electromagnetics Research Symposium (PIERS — Toyama)*, Toyama, Japan, Aug. 1–4, 2018.



4. Razevig, V. V., A. V. Zhuravlev, A. S. Bugaev, M. A. Chizh, and S. I. Ivashov, “Imaging under irregular surface using microwave holography,” *2017 Progress In Electromagnetics Research Symposium — Fall (PIERS — FALL)*, Singapore, Singapore, Nov. 19–22, 2017.
5. <https://video.repubblica.it/edizione/firenze/firenze-ecco-il-robot-che-individua-in-sicurezza-le-mine-antiuomo/317124/317755>.
6. Pochanin, G., L. Varianytsia-Roshchupkina, V. Ruban, I. Pochanina, P. Falorni, G. Borgioli, L. Capineri, and T. Bechtel, “Design and simulation of a “single transmitter-four receiver” impulse GPR for detection of buried landmines,” *2017 9th International Workshop on Advanced Ground Penetrating Radar (IWAGPR)*, 1–5, Edinburgh, Scotland, Jun. 28–30, 2017.
7. [https://en.wikipedia.org/wiki/Pearson\\_correlation\\_coefficient](https://en.wikipedia.org/wiki/Pearson_correlation_coefficient).
8. Pochanin, G., L. Capineri, T. Bechtel, P. Falorni, G. Borgioli, V. Ruban, O. Orlenko, T. Ogurtsova, O. Pochanin, F. Crawford, and P. Kholod, “Measurement of coordinates for a cylindrical target using times of flight from a 1-transmitter and 4-receiver UWB antenna system,” submitted to *IEEE Transactions on Geoscience and Remote Sensing*, (under revision).